Synthesis and optical properties of nanostructured $Ce(OH)_4$

Ansari A A† and Kaushik A

(National Physical Laboratory, Dr. K. S. Krishnan Marg, Pusa, New Delhi-110012, India)

Abstract: Nanocrystalline cerium hydroxide (NCs-$Ce(OH)_4$) is a intermediate product of CeO_2, synthesized successfully using a novel and simple wet chemical rout at an ambient temperature for the preparation of NCs CeO_2 powder and film on mass scale for various purposes. The synthesized NCs-$Ce(OH)_4$ was characterized using X-ray diffraction (XRD), scanning electron microscopy (SEM), thermo-gravimetric analysis (TGA), Fourier transform infrared (FTIR), UV-visible and photoluminescence (PL) spectroscopy. The average crystallite size of NCs-$Ce(OH)_4$ has been estimated by the Scherrer equation to be 3–4 nm. The SEM examinations show that the surface texture was uniformly agglomerated and homogeneous. Thermal analysis suggests that cerium (IV) ion is in the tetra hydrated form. Absorption and luminescence spectroscopic studies have been examined for future application in the development of optical devices.

Key words: NCs-$Ce(OH)_4$; X-ray diffraction; thermo-gravimetric analysis; optical properties
DOI: 10.1088/1674-4926/31/3/033001 **EEACC:** 2520

1. Introduction

Nanocrystalline (NCs) metal hydroxides have been intensively studied in recent decades, not only for their fundamental scientific interest but also for the different kinds of technological applications in applied sciences and material sciences owing to their size-dependent properties[1]. NCs materials show unique optical and electrical properties, which are derived from their low dimensionality, and possible quantum-confinement effects compared with macrocrystalline materials[2]. Properties such as electrical transport, lattice dynamic, optical and catalytic properties of NCs materials can be significantly enhanced by controlling their grain size in nanoscale[3]. These characteristics have created a new challenge for research in ion-conductive materials due to its important applications, such as gas sensors[4, 5], fuel cell technology[6], non-linear optics[7], catalytic, high electrical conductivity[2] and interaction between the solid and ambient atmosphere. Cerium oxide (ceria, CeO_2) is a rare earth oxide that has received a great deal of interest from researchers because of its unusual properties includes high chemical stability, high charge transfer capability, nontoxicity oxygen ion conductivity, oxygen storage capacity and biocompatibility[8]. Because of these novel properties, CeO_2 nanoparticles can be widely exploited for polishing agent and sensing applications on mass scale[5]. Therefore, it is necessary to develop some new methods for the industrial scale production of cerium oxide nanoparticles. For the extensive application of CeO_2 nanocrystals, an economical mass production method is urgently needed. The synthesis of CeO_2 nanoparticles is a multi step process and the particle size and reactivity of CeO_2 nanoparticles depends on the intermediate species, mainly $Ce(OH)_4$. It is noticed that the preparation of $Ce(OH)_4$ in the nanosize scale will provide a better way for the synthesis of CeO_2 nanoparticle on an industrial scale. Some techniques have been used for the synthesis of $Ce(OH)_4$ material but their NCs nature still remains challenging[9−11]. However, most of these techniques are multi step reaction, time taking, energy consuming, and not eco-friendly. However, the syntheses and optical properties of NCs-$Ce(OH)_4$ on a large scale is rarely reported.

In the present work, we synthesized NCs-$Ce(OH)_4$ using a simple wet chemical method and characterized by analytical techniques.

2. Experimental details

2.1. Preparation method

All chemicals such as $(NH_4)_2Ce(NO_3)_6$, NH_4OH and ethanol were of analytical grade and purchased from Merck India Ltd, Mumbai, India. The deionized water obtained from the Millipore water purification system (Milli Q 10 TS) was used for the preparation of solutions.

For the synthesis of NCs-$Ce(OH)_4$, $(NH_4)_2Ce(NO_3)_6$ and NH_4OH were used as starting precursors without any further purification. 5 mL of ammonium solution (1M) was added into 1.0 g ammonium cerium nitrate $[(NH_4)_2Ce(NO_3)_6]$ solution dissolved in 20 mL distilled water with constant stirring for 1 h. A gray color precipitate was achieved by the addition of ammonia solution. Excess ammonia solution was added drop-wise until pH 9.0 was achieved in the solution. The resulting mixture was left to stir continuously for a further 3 h to complete the reaction. After complete stirring a pale yellow precipitate of $Ce(OH)_4$ appeared, centrifuged and was washed several times with deionized water to remove excess ammonium and nitrate ions from the solution mixture. Washed yellow precipitate was dried in the oven at 100 ℃ to remove the excess water.

During the synthesis of $Ce(OH)_4$, we examined systematic changes in the color of the precipitate. The color of the precipitate changed gradually from gray to yellow after being exposed to air, maybe due to the oxidation of peroxide $Ce(OH)_3OOH$ to $Ce(OH)_4$ by oxygen[10]. Previous reports have been suggested that only CeO_2 and $Ce(OH)_4$ are of this color, and the others are colorless[12−15]. The process is however slow due to the low oxygen concentration ($\sim 10^{-5}$) in normal ambient condi-

† Corresponding author. Email: aneesaansari@gmail.com
Received 19 October 2009, revised manuscript received 14 November 2009

tions. The reaction for the preparation of $Ce(OH)_4$ is given by the following equations.

$$(NH_4)_2Ce(NO_3)_6 + 4NH_4OH + H_2O \xrightarrow{70\ ^\circ C} Ce(OH)_3OOH + 6NH_4NO_3 + 2H^+,$$

$$Ce(OH)_3OOH + 2H^+ \rightarrow Ce(OH)_4 + H_2O.$$

2.2. Characterization techniques

X-ray diffraction (XRD, CuKa radiation (Rigaku) studies have been done to identify the crystal structure of prepared $Ce(OH)_4$ powder. Scanning electron microscopy (SEM, LEO-440) studies have been conducted to examine the surface morphology. The absorption spectra of the NCs-$Ce(OH)_4$ and bulk CeO_2 powder were measured using the UV/Vis spectrophotometer in the wavelength range from 200–600 nm. The fourier transform infrared (FTIR) spectra of NCs-$Ce(OH)_4$ have been recorded using the FTIR (Perkin-Elmer) spectrophotometer, using KBr pellets, in the range of 400 to 4000 cm^{-1}. Thermogravimetric analysis was measured on a Perkin-Elmer TGA instrument in nitrogen atmosphere at a heating rate of 20 °C/min. Photoluminescence (PL) spectra were measured using Perkin-Elmer L-55 luminescence spectrometer.

3. Results and discussion

Figure 1 shows the X-ray diffraction pattern of $Ce(OH)_4$ powder prepared by co-precipitation method. XRD pattern shows all reflection planes resemble the JCPDS standard data[11] and confirm the crystallinity and high phase purity of $Ce(OH)_4$. The X-ray diffractograms (in the range 2θ, 10–70 °C) of the film show a presence of (111), (200), (220) and (331) reflection planes corresponding to a cubic fluorite structure of $Ce(OH)_4$. The average crystallite size of $Ce(OH)_4$ particles estimated according to Scherrer's formula is 3–4 nm. However, broadening in reflection planes indicates NCs nature of the particles.

Figure 2 shows SEM micrograph of NCs-$Ce(OH)_4$ powder. The SEM image of $Ce(OH)_4$ reveals that the particles are highly agglomerated and uniformly distributed. This may be due to the small grain size and the presence of bulky hydroxyl groups.

The thermogram of NCs-$Ce(OH)_4$ was recorded from ambient temperature to 700 °C as shown in Fig. 3. The main objective of the thermal analysis to assign the number and nature of the hydroxyl molecule(s) present in the NCs-$Ce(OH)_4$ molecule.The TGA spectrum shows first inflexion point, started from 30 °C and completed at 120 °C with the weight loss 15%, which is equivalent to the removal of 2-hydroxyl molecule (calculated weight loss for one H_2O molecule and one hydroxyl molecules is 16.8%). Continuous weight loss below 100 °C indicates that one water molecule is present in the outer coordination sphere, whereas continuous weight loss above 100 °C is due to the removal of the hydroxyl molecule that is present in the inner coordination sphere. The second inflexion point is observed in the temperature range from 120 to 464 °C, shows a weight loss of 23% and represents the elimination of three-hydroxyl molecules (calculated weight loss for one hydroxyl molecule is 24.50%). The expulsion of a hydroxyl molecule at such a higher temperature could be related to the steric repulsion caused by three-hydroxyl molecule and f-orbital of cerium. The TGA analysis reveals that cerium

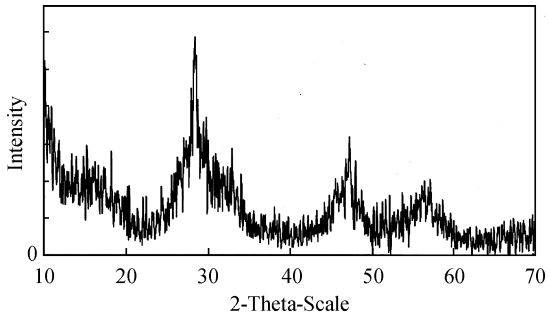

Fig. 1. X-ray diffraction pattern of NCs-$Ce(OH)_4$ powder.

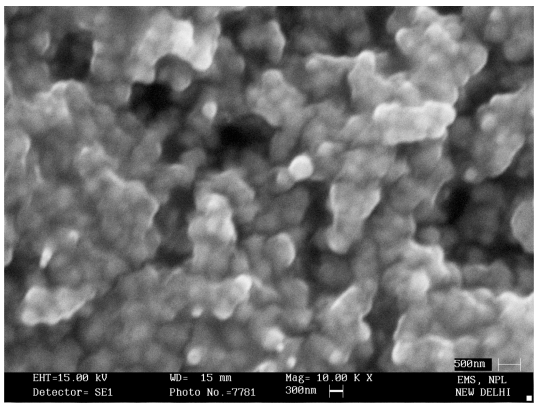

Fig. 2. Scanning electron micrograph of NCs-$Ce(OH)_4$ powder.

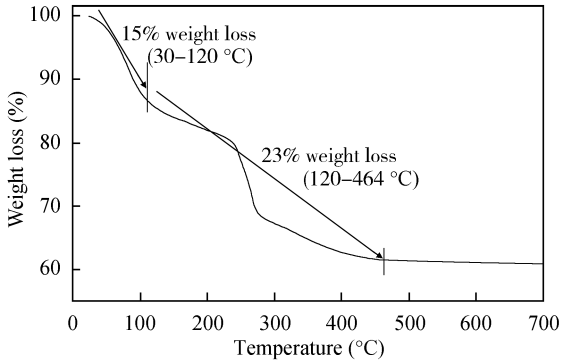

Fig. 3. Thermo-gravimetric analysis of NCs-$Ce(OH)_4$ powder.

is in tetra-hydrated form and also suggests the redox behavior of cerium ion, which is changing according to temperature.

Figure 4 shows the FTIR absorption spectra of NCs-$Ce(OH)_4$ along with bulk CeO_2 powder. An infrared band observed at 3148 cm^{-1} assigned to O–H stretching mode indicating the presence of hydroxyl group, which are disappeared in the bulk CeO_2 powder. The infrared band corresponds to the OH group of $Ce(OH)_4$ and is approximately four times more intensive than that of CeO_2. This drastic enhancement in the intensity corresponds to the OH vibration mode confirmed by the presence of a large number of OH group. The infrared band of $Ce(OH)_4$ shows the sharp OH vibration bands are characteristic of true hydroxide this is correlated with TGA analysis. The appearance of a sharp and intense band at 523 cm^{-1} is assigned to the Ce–O stretching vibration mode indicating the formation

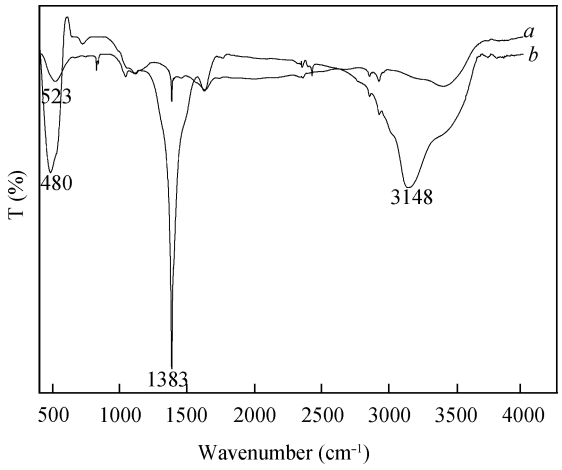

Fig. 4. FTIR spectra of (*a*) bulk CeO_2 powder and (*b*) NCs-$Ce(OH)_4$ powder.

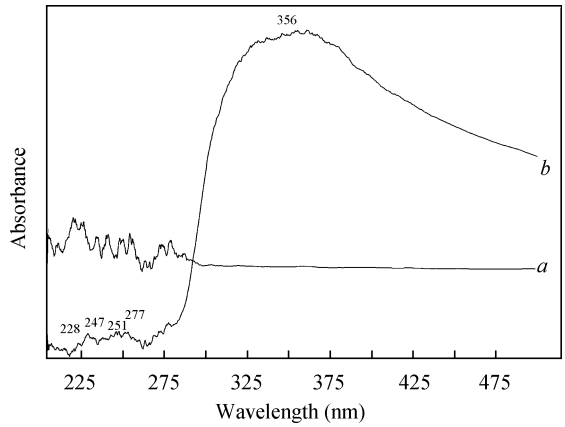

Fig. 5. Absorption spectra of (*a*) bulk CeO_2 powder and (*b*) NCs-$Ce(OH)_4$ powder.

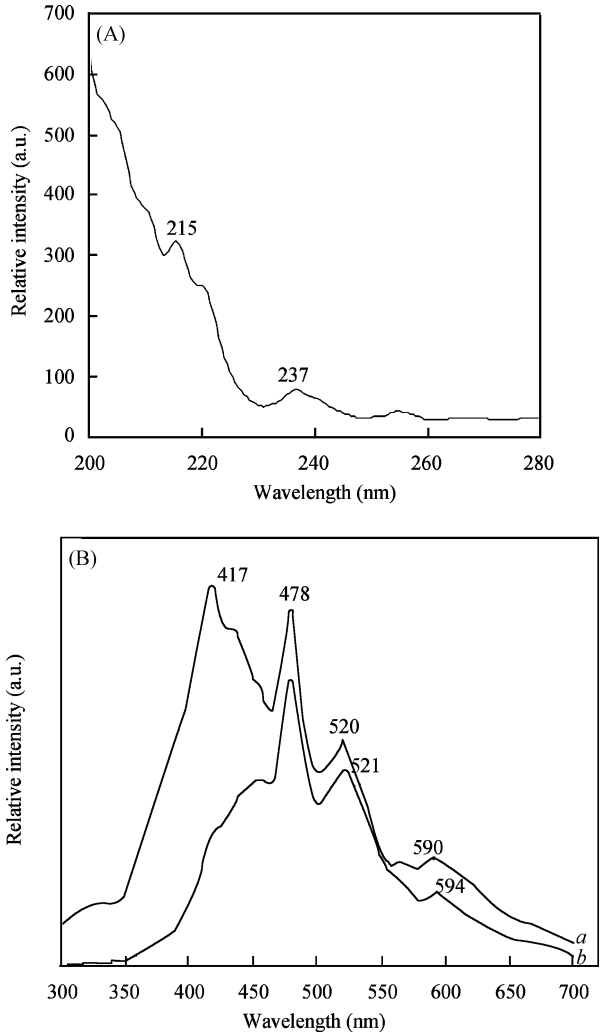

Fig. 6. Photoluminescence spectra of (A) excitation spectra of NCs-$Ce(OH)_4$ and (B) (*a*) bulk CeO_2 powder and (*b*) NCs-$Ce(OH)_4$ powder.

of $Ce(OH)_4$[16].

Figure 5 shows absorption spectra of NCs-$Ce(OH)_4$ along with bulk CeO_2 powder (reflectance mode). UV-visible absorption spectra of NCs-$Ce(OH)_4$ shows absorption peaks at 214, 220, 247, 251, 277 and 356 nm[17−19] which are identical to their bulk counterpart (CeO_2). The absorption bands are shifted towards a lower wavelength due to the decreasing grain size of the material ($Ce(OH)_4$) and increasing charge transfer gap between the 2p orbital of O and 4f orbital of Ce^{4+} bonds compared with bulk CeO_2[18, 19]. A broad absorption band is observed in the wavelength range from 300 to 500 nm (Fig. 5(a)). This may be due to the charge transfer transition from O^{2-} (2p) to Ce^{4+} (4f) orbital in $Ce(OH)_4$. The Uv-Vis absorption spectra also suggests that the local environment of $Ce(OH)_4$ and CeO_2 is similar but $Ce(OH)_4$ is more structurally disordered in respect to CeO_2[20]. Since the spin-orbit components of the excited cerium 5d state, $^2D_{5/2}$ and $^2D_{3/2}$, are strongly split by the crystal field effect[21, 22]. The bands were consistent with reported data for f–d electron transitions in cerium and indicated that useful optical properties were retained in the NCs materials[17−19, 22].

Figure 6 shows the photoluminescence spectra of bulk CeO_2 and NCs-$Ce(OH)_4$ excited at 250 nm wavelength. The PL spectra $Ce(OH)_4$ nanoparticles shows a significant difference in emission band in comparison of bulk CeO_2. It is shown that the bulk spectrum of CeO_2 exhibits broad emission band maxima at 417 nm and some other bands maxima at 478, 520 and 590 nm respectively. These well resolved peaks in the luminescence spectrum corresponds to the direct emission from the 2D($5d^1$) state to the two split $4f^1$ ground states of $^2F_{5/2}$ and $^2F_{7/2}$ caused by spin orbit coupling[22]. This splitting for Ce^{3+} in the current bulk CeO_2 are due to the macro crystal size effect. There is a broad emission band at 417 nm that is remarkably diminished and merged in a broad emission band with maxima at 479 nm (Fig. 6(b)). The emission efficiency of the $Ce(OH)_4$ nanoparticles is relatively low corresponding to their bulk CeO_2 this may be due to the quenching effect. This quenching phenomenon is due to the presence of bulk hydroxyl groups at the surface of the nanoparticles, which are efficient non-radiative recombination centers: their elimination by deuteration induces an increase of the luminescence[23]. These results are explained by an increase of the Ce^{4+} content in the naqnoparticles, which is known to efficiently quench the emission of the bulk powder[19, 23]. However, a very small red shift of the emission band towards a longer wavelength which

may be due to the presence of a small amount of Ce^{3+} on the surface of $Ce(OH)_4$ nanoparticles. Furthermore, it is interesting that the emission spectrum of $Ce(OH)_4$ nanoparticles is greatly different from the spectrum of bulk CeO_2 powder and caused by the charge transfer transition from O^{2-} to Ce^{4+}.

4. Conclusions

NCs-$Ce(OH)_4$ was successfully synthesized using the wet chemical route at ambient temperature. Significant optical properties of NCs-$Ce(OH)_4$ material were measured which are different from their bulk counterpart. The synthetic procedures described in this study offer several important advantages for the production of CeO_2 nanocrystals on mass scale for industrial purposes. The SEM micrographs of prepared $Ce(OH)_4$ nanoparticles show that the particles were in a highly agglomerated form and had a length of 3–4 nm in size, confirmed by the XRD pattern. Efforts are being made to improve the quality of the powder for application to luminescent device fabrication and solar cell materials.

Acknowledgement

The authors (AAA) would like to thank CSIR for financial support and the Director of NPL for providing experimental facilities, which is gratefully acknowledged.

References

[1] Yu T, Joo J, Park Y I, et al. Large-scale nonhydrolytic sol-gel synthesis of uniform-sized ceria nanocrystals with spherical, wire, and tadpole shapes. Angew Chem Int Ed, 2005, 44(45): 7411

[2] Suzuki T, Kosacki I, Anderson H U. Electrical conductivity and lattice defects in nanocrystalline cerium oxide thin films. J Am Ceram Soc, 2001, 84(9): 2007

[3] Zheng X, Zhang X, Fang Z, et al. Characterization and catalysis studies of CuO/CeO_2 model catalysts. Cataly Commun, 2006, 7(9): 701

[4] Trinchi A, Li Y X, Wlodarski W, et al. Investigation of sol–gel prepared CeO_2–TiO_2 thin films for oxygen gas sensing. Sensors and Actuators B, 2003, 95(1–3): 145

[5] Barreca D, Gasparotto A, Maccato C, et al. Columnar CeO_2 nanostrcrures for sensor application. Nanotechnology, 2007, 18(12): 125502

[6] Turkovic A, Orel Z C. Dye-sensitized solar cell with CeO_2 and mixed CeO_2/SnO_2 photoanodes. Solar Eng Mater Sol Cells, 1997, 45(3): 275

[7] Ho C, Yu J C, Kwang T, et al. Morphology-controllable synthesis of mesoporous CeO_2 nano- and microstructures. Chem Mater, 2005, 17(17): 4514

[8] Dutta P, Pal S, Seehra M S, et al. Concentration of Ce^{3+} and oxygen vacancies in cerium oxide nanoparticles. Chem Mater, 2006,18(21): 5144

[9] Tok A I Y, Boey F Y C, Dong Z, et al. Hydrothermal synthesis of CeO_2 nanoparticles. J Mater ProcTech, 2007, 190(3): 217

[10] Tang C, Bando Y, Liu B, et al. Cerium oxide nanotubes prepared from cerium hydroxide nanotubes. Adv Mater, 2005, 17(24): 3005

[11] Balasubramaniana M, Melendresa C A, Mansour A N. An X-ray absorption study of the local structure of cerium in electrochemically deposited thin films. Thin Solid Films, 1999, 347(2): 178

[12] Decroly A, Petitjean J P. Study of the deposition of cerium oxide by conversion on to aluminium alloys. Surf & Coating Technol, 2005, 194(1): 1

[13] Golden T D, Wan A Q. Anodic electrodeposition of cerium oxide thin films. J Electrochem Soc, 2003,150(9): C621

[14] Li F, Yu X, Pan H, et al. Syntheses of MO_2 (M = Si, Ce, Sn) nanoparticles by solid-state reactions at ambient temperature. Solid State Sci, 2000, 2(8): 767

[15] Patil R K, Lee I C, Gaskell K J, et al. Precipitation of nanocrystalline CeO_2 using triethanolamine. Langmuir, 2009, 25(1): 67

[16] Gu H, Soucek M D. Preparation and characterization of monodisperse cerium oxide nanoparticles in hydrocarbon solvents. Chem Mater, 2007, 19(5): 1103

[17] Wang Z, Quan Z, Lin J. Remarkable changes in the optical properties of CeO_2 nanocrystals induced by lanthanide ions doping. Inorg Chem, 2007, 46(13): 5237

[18] Wang Z L, Quan Z W, Jia P Y, et al. A facile synthesis and photoluminescent properties of redispersible CeF_3, CeF_3:Tb^{3+}, and CeF_3:Tb^{3+}/LaF_3 (Core/Shell) nanoparticles. Chem Mater, 2006, 18(8): 2030

[19] Xing Y, Li M, Davis S A, et al. Synthesis and characterization of cerium phosphate nanowires in microemulsion reaction media. J Phys Chem B, 2006, 110(3): 1111

[20] Patil S, Seal S, Guo Y, et al. Role of trivalent La and Nd dopants in lattice distortion and oxygen vacancy generation in cerium oxide nanoparticles. Appl Phys Lett, 2006, 88(25): 243110

[21] Brus L E. Electronic wavefunctions in semiconductor clusters. J Phys Chem, 1986, 90: 2555

[22] Tang C, Bando Y, Golberg D, et al. Cerium phosphate nanotubes: synthesis, valence state, and optical properties. Angew Chem Inter Ed, 2005, 44(4): 576

[23] Buissette V, Moreau M, Gacoin T, et al. Colloidal synthesis of luminescent rhabdophane $LaPO_4$:$Ln^{3+}\cdot xH_2O$ (Ln = Ce, Tb, Eu; $x \approx 0.7$) nanocrystals. Chem Mater, 2004,16(19): 3767